Latent superconductivity at parallel interfaces in a superlattice dominated by another collective quantum phase

V. N. Moura,[1,*] Davi S. Dantas,[1] G. A. Farias,[1] A. Chaves,[1,2] and M. V. Milošević[2,†]

[1]*Departamento de Física, Universidade Federal do Ceará, Caixa Postal 6030, Campus do Pici, 60455-900 Fortaleza, Ceará, Brazil*

[2]*Department of Physics, University of Antwerp, Groenenborgerlaan 171, B-2020 Antwerp, Belgium*

(Received 14 October 2021; revised 6 May 2022; accepted 6 July 2022; published 22 July 2022)

We theoretically examine behavior of superconductivity at parallel interfaces separating the domains of another dominant collective excitation, such as charge density waves or spin density waves. Due to their competitive coupling in a two-component Ginzburg-Landau model, suppression of the dominant order parameter at the interfacial planes allows for nucleation of the (hidden) superconducting order parameter at those planes. In such a case, we demonstrate how the number of the parallel interfacial planes and the distance between them are linked to the number and the size of the emerging superconducting gaps in the system, as well as the versatility and temperature evolution of the possible superconducting phases. These findings bear relevance to a broad selection of known layered superconducting materials, as well as to further design of artificial (e.g., oxide) superlattices, where the interplay between competing order parameters paves the way towards otherwise unattainable superconducting states, some with enhanced superconducting critical temperature.

DOI: 10.1103/PhysRevB.106.014516

I. INTRODUCTION

Controlling and enhancing the thresholds of superconducting (SC) phase have been challenging physicists since the very discovery of superconductivity. Over the past decades, different approaches have been proposed to enhance the critical temperature T_c of different superconducting materials by, for instance, reducing the sample dimensionality [1–4], curving its surface [5], applying shear strain effects [6], or by imposing hydrostatic pressure [7–10]. Understanding and tailoring the mechanism behind the unconventional high-T_c superconductivity, exhibited by cuprates and iron pnictides, for example, may provide additional pathways to enhance the temperature domain of the superconducting phase. In these materials, the high critical temperature is intimately connected with the interplay between different collective quantum states, namely, charge and spin density waves and the superconducting state [11–14]. These additional ordered quantum phases may suppress superconductivity by competing for the same electrons wrapped in the Cooper-pairing mechanism, but may also assist Cooper pairing through, e.g., coupling between charge-ordered states and the crystal lattice vibrations, enhancing the superconducting state [13]. In fact, unlike conventional superconductivity, where the pairing mechanism is mediated solely by the phonon interaction, in high-T_c superconductors the superconducting ground state is formed in presence of strong fluctuations of the charge- and spin-ordered states as discussed in Ref. [15].

The coexistence of superconductivity and other collective states has been experimentally observed in several materials, such as in Na(Fe,Co)As [14], in the underdoped $Ba(Fe_{0.953}Co_{0.047})_2As_2$ compound [16], in $(Ba,K)Fe_2As_2$ systems [17], in $LaPt_2(Si,Ge)_2$ [18,19], $La_{2x}Sr_xCuO_4$ [20,21], in the quasi-one-dimensional material $HfTe_3$ [22], in Pd-doped 2H-$TaSe_2$ [23], $2H-TaSe_2$ under pressure [24], in $NbSe_2$ films [25], etc. Aside from the bulk-layered materials, the coexistence or competition of quantum phases in the context of superconductivity is highly relevant to artificially composed superlattices, be it thin films [26,27], consecutive oxide interfaces [28,29], or van der Waals heterostructures [30,31]. Even within selected monolayer two-dimensional (2D) materials [especially transition-metal dichalcogenides (TMDs)] [25,32], competition of quantum phases is expected, strongly dependent on the sample thickness [33]. In that context, in a recent work a two-component Ginzburg-Landau (GL) approach along with an extension of McMillan theory has been used to describe the interplay between charge density waves (CDW) and superconducting phases in layered TMDs [34]. Using a similar GL model, a more general analysis was provided by Moor *et al.* [35] to describe the rise of interface superconductivity as a hidden order parameter only at the interface between two separate regions where another collective phenomenon, such as charge and spin density wave, is dominant. However, a model where superconductivity rises at several parallel interfaces, which is a case of practical interest [28–31], requires an extension of the single interface model developed in Ref. [35] that has yet to be properly developed, in order to allow one to investigate the role of interface coupling on parameters such as superconducting critical temperatures and Cooper-pair densities at the interfaces.

In this paper, motivated by many (bulk or artificial) layered systems where competition of superconductivity with other quantum orders is relevant, we apply the two-component GL model to address physics stemming from the proximity of

*victornocrato@fisica.ufc.br

†milorad.milosevic@uantwerpen.be

parallel material interfaces. We investigate how the controllable geometric parameters of the system, such as the number of parallel interfaces and the distance between them, can be used to tune the possible superconducting states and the overall critical temperature of interface superconductivity competing with another bulk order. Our results demonstrate the existence of "bands" of emerging superconducting gaps (i.e., range of achievable critical temperatures) as the number of parallel interfaces (translating to the thickness of the overall system) is increased. Furthermore, we establish thresholds for the constructive or destructive crosstalk of superconducting order between the adjacent interfaces, and show different states emerging when manipulating the distance between interfaces, each with different temperature dependence and different contribution to the overall critical temperature of the system as a whole.

The paper is organized as follows. In Sec. II, we present the theoretical framework for the study of interface superconductivity in a system with competing density wave (DW) and SC order parameters, within the linearized and the fully nonlinear GL formalism. In Sec. III, we detail the eigenfunctions and eigenvalues of the linearized equations for the SC order parameter, where we also propose an approximate minimal tight-binding model that allows one to predict results for an arbitrary number of parallel interfaces. Results obtained using the full nonlinear two-component GL approach are discussed in Sec. IV. Our main findings and conclusions are summarized in Sec. V.

II. THEORETICAL MODEL

We consider two order parameters Δ and W describing, respectively, a (hidden) superconducting phase and another collective excitation, such as CDW or spin density wave (SDW). The corresponding two-component Ginzburg-Landau (GL) free energy F is then defined as

$$F = \int dx \Big\{ \xi_s^2 (\nabla\Delta)^2 - \alpha_s \Delta^2 + \frac{\beta_s}{2}\Delta^4 + \xi_{\rm w}^2 (\nabla W)^2 - \alpha_{\rm w}(x) W^2 + \frac{\beta_{\rm w}}{2} W^4 + \gamma W^2 \Delta^2 \Big\}, \quad (1)$$

where $\alpha_{\rm w}$ and $\beta_{\rm w}$ are the usual phenomenological expansion parameters in the derivation of the GL formalism, while γ is the coupling between condensate densities. This free energy can be written in a dimensionless form $\mathscr{F}$ as

$$\mathscr{F} = \int dx \Big\{ \frac{1}{\delta^2}(\nabla\Delta)^2 + \frac{\xi_r^2}{\delta^2}\Big[-\alpha_s \Delta^2 + \frac{1}{2}\Delta^4 \Big] + (\nabla W)^2 - \Omega_{\rm w}(x) W^2 + \frac{1}{2} W^4 + \sigma W^2 \Delta^2 \Big\}, \quad (2)$$

where unit of energy is $F_0 = \alpha_{\rm w0}^2/\beta_{\rm w}$ ($\alpha_{\rm w0}$ is the density wave parameter $\alpha_{\rm w}$ in the bulk), and $\delta = W_{\rm b}/\Delta_{\rm b}$, with $W_{\rm b}$ and $\Delta_{\rm b}$ as the maximum values of the respective order parameters. The coefficient $\xi_r^2 = \xi_{\rm w}^2/\xi_s^2$ relates the coherence lengths $\xi_{\rm w} = \hbar/\sqrt{2m\alpha_{\rm w0}}$ and $\xi_s = \hbar/\sqrt{2m\alpha_s}$ of the (charge and spin) density wave (DW) and superconducting phases, respectively, $\sigma = \gamma\delta^2/\alpha_{\rm w0}$, and $\alpha_s = 1 - T/T_\Delta$, where T_Δ is the bulk critical temperature of the superconducting phase. $\xi_{\rm w}$ is taken as the unit for distances and for the space coordinate x. The parameter $\Omega_{\rm w}(x)$ is used to induce suppression of $W(x)$ at the interfaces, such that

$$\Omega(x) = \begin{cases} -\alpha_0, & |x - \chi_j| < L \\ +1, & |x - \chi_j| \geqslant L \end{cases} \quad (3)$$

where $\alpha_0 \geqslant 0$, L is the width of the interfacial regions, and χ_j ($j = 1, 2, 3, \ldots, N$) is the position of the jth interface in a system with N interfaces.

Minimizing $\mathscr{F}$ with respect to Δ and W leads to two coupled Ginzburg-Landau equations

$$-\frac{d^2W}{dx^2} + [-\Omega_{\rm w}(x) + W^2 + \sigma\Delta^2]W = 0, \quad (4)$$

$$-\frac{1}{\xi_r^2}\frac{d^2\Delta}{dx^2} + \Big[-\alpha_s + \Delta^2 + \frac{\sigma\delta^2}{\xi_r^2} W^2 \Big]\Delta = 0. \quad (5)$$

Even though the numerical solution of Eqs. (4) and (5), based on a self-consistent relaxation procedure, will be eventually provided in Sec. IV, we will also discuss here the solutions based on the following linearized GL formalism, to gain insights in the physics behind the complete solution of the system of GL equations. Assuming a weak superconducting gap at the interface, higher-order terms in Δ can be neglected in Eqs. (4) and (5), so that [35]

$$-\frac{d^2W}{dx^2} + [-\Omega_{\rm w}(x) + W^2]W = 0, \quad (6)$$

$$-\frac{1}{\xi_r^2}\frac{d^2\Delta}{dx^2} + \Big[-\alpha_s + \frac{\sigma\delta^2}{\xi_r^2} W^2 \Big]\Delta = 0. \quad (7)$$

Equation (6) is then discretized on a uniform Cartesian grid (with spacing $0.1\,\xi_{\rm w}$) in a finite-difference scheme and numerically solved by means of a relaxation method. An initial (arbitrary) trial function for $W(x)$ evolves in time as

$$W_i^{t+1} = W_i^t + dt\Big[\frac{W_{i+1}^t - 2W_i^t + W_{i-1}^t}{dx^2} - \Omega_{\rm w}^i W_i^t + (W_i^t)^3 \Big], \quad (8)$$

with a (dimensionless) time step $dt = 0.01$, until convergence is reached up to tolerance $|W_i^{t+1} - W_i^t| \leqslant 10^{-8}$ at any point in space x_i. The converged solution for $W(x)$ is then used as input in Eq. (7),

$$-\frac{d^2\Delta}{dx^2} + \sigma\delta^2 |W|^2 \Delta = \varepsilon\Delta, \quad (9)$$

where $\varepsilon = \xi_r^2\alpha_s$ and the equation is discretized in the same spatial grid. Notice the resemblance of this equation with Schrödinger equation for a $\sigma\delta^2|W(x)|^2$ potential. We numerically solve this eigenvalue equation, which yields a series of solutions for the superconducting order parameter, each with an eigenvalue ε_n and a gap distribution $\Delta_n(x)$ that is nonzero at the interfacial regions, thus describing interface superconducting states. This situation is sketched in Fig. 1, illustrating the suppressed $W(x)$ and increased $\Delta(x)$ at a pair of parallel interfaces. Given the temperature dependence of α_s and the value of ξ_r^2, one can obtain the critical temperature T_{cn} for the nth superconducting eigenstate of this system, as we will demonstrate in what follows. Alternatively, one can solve Eq. (7) through a relaxation procedure for different temperatures, to reveal the temperature dependence of $\Delta_n(x)$. The full solution of the nonlinearized GL equtions (4) and

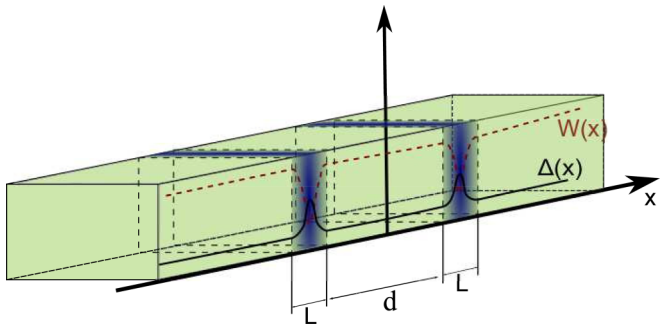

FIG. 1. Sketch of a system with two adjacent interfaces, based on the single-interface system proposed in Ref. [35]. Here, the order parameter $W(x)$ (dashed line) describes a collective excitation (e.g., spin or charge density waves) dominating in the bulk (green), that is suppressed along parallel interfaces (blue) of width L, separated by distance d [see Eq. (3)]. The hidden order parameter $\Delta(x)$, which describes the superconducting phase, arises at these interfaces (plotted as a solid line).

(5), to be discussed in Sec. IV, is also obtained by the same relaxation procedure, assuming convergence is achieved as the error reaches $|\Delta_i^{t+1} - \Delta_i^t| \leqslant 10^{-11}$ at any point in space x_i.

In general, the model proposed here is applicable to superconductors with coexisting SDW, such as Fe-based pnictides, as well as to those with a CDW, or cuprates. The correspondence between the $\alpha_{s(w)}$, $\beta_{s(w)}$, and γ paramaters in Eq. (1) and the microscopic parameters for these materials is discussed in Refs. [35–39]. However, a proper application of such a phenomenological model, as the one in Eq. (1), to these materials is currently not possible, due to the lack of experimental data on the spatial dependence of the order parameters involved in our model for actual samples in the literature [35]. Therefore, in what follows, all discussions will be made in terms of dimensionless units and conclusions will be mostly drawn in a qualitative way.

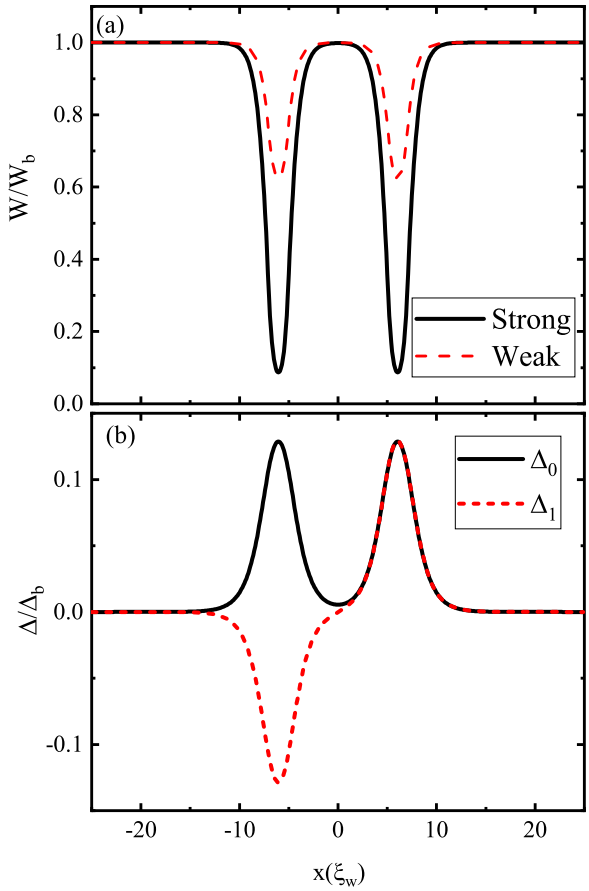

FIG. 2. Spatial distribution of the order parameters (a) of the density wave W, assuming its strong ($\alpha_0 = 5$, solid line) and weak ($\alpha_0 = 1$, dashed line) suppression at the interfaces, and (b) lowest-lying eigenfunctions of the SC state Δ_n in the strong DW suppression case, for two interfaces of width $L = 2\,\xi_w$, separated by $d = 12\,\xi_w$ (cf. Fig. 1).

III. INTERFACE EIGENSTATES AND THEIR CRITICALITY

To begin with, we recall that Ref. [35] readily contains an extensive study of the single interface case, and shows that the eigenstates of Eq. (9) represent different possible distributions of the superconducting order parameter $\Delta(x)$, each with a different eigenvalue (critical temperature) ε_n, which are reminiscent of the eigenstates of the Schrödinger equation for a particle confined in a quantum well.

We therefore start our analysis from one pair of parallel interfaces. In what follows, all interfaces will have the same width $L = 2\,\xi_w$, where the ground state of each interface is well separated in energy from the first excited state, thus allowing us to interpret the behavior of the system only using the ground state of the SC order parameter in each interface. The density wave $W(x)$ and superconducting $\Delta(x)$ order parameters in this case are shown in Figs. 2(a) and 2(b), respectively. The two interfaces are separated by distance $d = 12\,\xi_w$, and we assume $\xi_r = 1.0$ (i.e., $\xi_s = \xi_w$). Notice the two dips in $W(x)$, calculated by Eq. (8) with $\Omega(x)$ given by Eq. (3) with $\chi_1 = -6\,\xi_w$ and $\chi_2 = +6\,\xi_w$, exactly at the position of the interfaces, representing suppression of the DW phase at these regions. Increasing the value of α_0 then leads to a stronger suppression of the order parameter W. We consider $\alpha_0 = 1$ for a weak DW suppression, and $\alpha_0 = 5$ for strong suppression. The two lowest-lying eigenfunctions of the SC order parameter in the $\alpha_0 = 5$ case peak at the interfaces, thus representing the rise of interface superconductivity. The symmetric and antisymmetric characters of these solutions are reminiscent of the double-quantum-well problem.

As in a double quantum well, the eigenvalues of Eq. (9) are expected to be degenerate if the interfaces are sufficiently far from each other (i.e., $d \to \infty$), whereas this degeneracy is lifted as they are brought closer to each other. This is exactly shown in Fig. 3, representing the eigenvalues ε of the SC states with symmetric (black solid) and antisymmetric (red dashed) eigenfunctions. One easily verifies that even a small suppression of the DW order gives rise to interface superconductivity. Interestingly, the dependence of the eigenvalues on the distance between interfaces d is affected by how strongly the DW phase is suppressed at the interfaces. As shown in Fig. 3(a), when the DW order is strongly suppressed, a sharp kink appears at $d = 2\,\xi_w$. Similar features are observed in

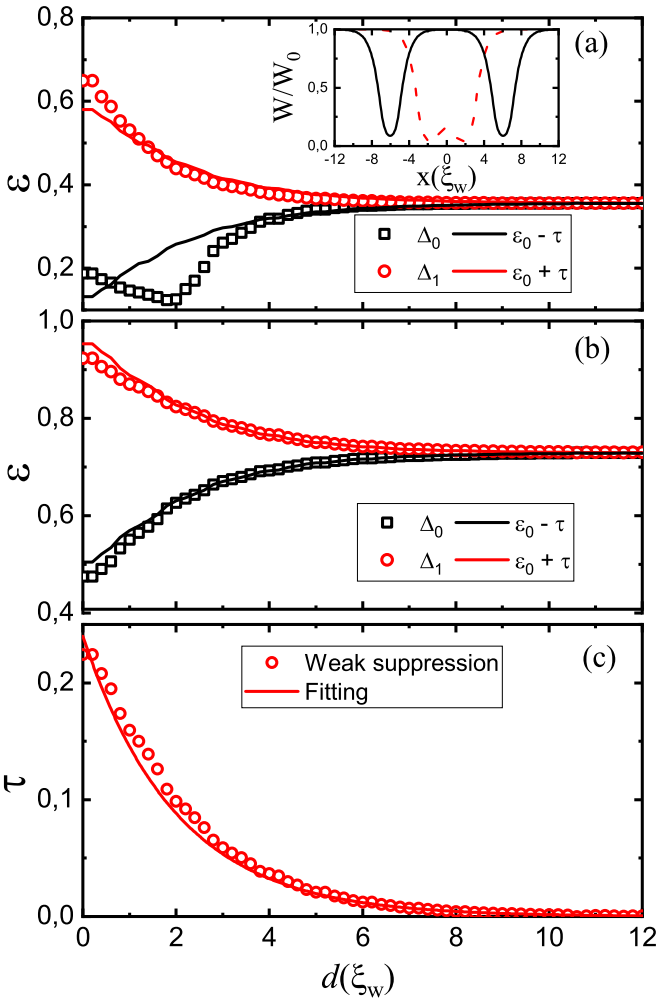

FIG. 3. Eigenvalues of Eq. (9) as a function of distance d between two interfaces, assuming strong (a) and weak (b) suppression of the DW order parameter W, i.e., with $\alpha_0 = 5$ and 1, respectively. Lines show the numerically obtained results for symmetric (black solid) and antisymmetric (red dashed) eigenfunctions, while open symbols plot results of a tight-binding approach for the same states. (c) The calculated hopping parameter τ as a function of distance d for a weak suppression case (open symbols), with an analytical fitting function plotted as well (solid curve). Inset in (a) shows the DW order parameter with $\alpha_0 = 5$ assuming $d = 4\xi_W$ (red dashed) and $d = 6\xi_W$ (black solid).

systems with more interfaces as well, as will be discussed later.

In fact, in the case where α_0 in Eq. (3) is set to a high value to produce strong DW suppression at the interfaces, as the distance between interfaces is made shorter, the DW order parameter no longer reaches its maximum value in the region between adjacent interfaces. This is shown in the inset of Fig. 3(a), which shows $W(x)$ for the two parallel interfaces system, assuming two values for the distance between the interfaces. One notices that for $d < 2\,\xi_w$, in the case of strong suppression, the crosstalk between the suppressions of the DW order parameter at the interfaces suppresses the order parameter between the interfaces as well, creating effectively a single region of weakly modulated DW order parameter.

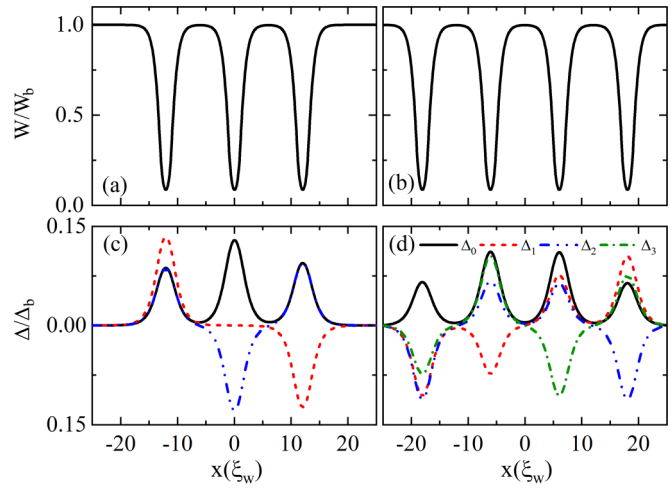

FIG. 4. DW order parameter W for a system consisting of (a) 3 and (b) 4 parallel interfaces, separated by distance $d = 12\,\xi_w$. The SC order parameters Δ_n of the first 3 and 4 low-lying eigenstates of these systems are shown in (c) and (d), respectively.

This maximizes the induced superconducting order parameter Δ. For further shortened distance d the area of (nearly fully) suppressed DW order is reduced, reducing the maximal emergent Δ.

The lift of the eigenstate's degeneracy, observed in Figs. 3(a) and 3(b), allows us to propose an approximate tight-binding model for the system, where we rewrite the eigenvalue equation (9) as $D\Delta = \varepsilon\Delta$, and the eigenvalues are obtained simply by diagonalization of the matrix D with diagonal terms given by the ground-state eigenvalue of each interface, $D_{11} = D_{22} = \varepsilon_0$, and the off-diagonal terms $D_{21} = D_{12} = -\tau$, where the latter plays the role of a hopping parameter between the adjacent interfaces. Diagonalization of D leads to eigenvalues $\varepsilon_\pm = \varepsilon_0 \pm \tau$ along with symmetric and antisymmetric eigenfunctions, qualitatively similar to those shown in Fig. 2(b). The hopping parameter τ increases as the distance d between interfaces decreases, thus controlling the separation between eigenvalues. Results of this model are shown as open symbols in Figs. 3(a) and 3(b), where very good agreement with the actual numerical results is verified in the case of weak suppression. In the strong suppression case, the made approximation and its results are describing the numerical data very well for larger interface separations.

The dependence of the hopping parameter τ on the interface separation d is plotted as open symbols in Fig. 3(c) for the weak suppression case. In order to facilitate the practical use of the tight-binding model proposed here, the numerically obtained hopping parameters are fitted by the function

$$\tau(d) = \tau_{\max} e^{-\frac{d}{2}}. \tag{10}$$

The fitting function is plotted as a solid curve in Fig. 3(c), using $\tau_{\max} = 0.24$. The importance of such a simplistic model as a convenient way to estimate the eigenvalues of Eq. (9) for any number of interfaces will be discussed further on.

We next proceed with the case of multiple parallel interfaces. The DW order parameter $W(x)$ is shown in Figs. 4(a) and 4(b), for a system consisting of 3 and 4 parallel

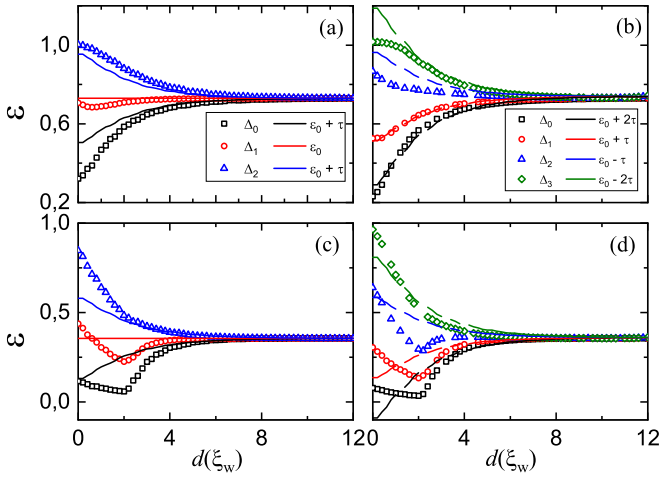

FIG. 5. Eigenvalues of the SC order parameter, from Eq. (9), assuming (a), (b) weak and (c), (d) strong DW suppression, in a system with (a), (c) 3 and (b), (d) 4 interfaces. For separation larger than $d \approx 4\,\xi_w$, the tight-binding model (symbols) predicts the eigenvalues reasonably well in all cases.

interfaces, respectively, separated by $d = 12\,\xi_w$. The first 3 and 4 low-lying eigenfunctions $\Delta_n(x)$ are shown in Figs. 4(c) and 4(d) for 3 and 4 interfaces, respectively. Interestingly, different eigenvalues produce eigenfunctions $\Delta_n(x)$ describing higher superconducting gaps at specific interfaces. For example, considering four interfaces, Δ_0 and Δ_3 (Δ_1 and Δ_2) states exhibit higher peaks at the two internal (external) interfaces. This suggests that, as the temperature of the system is decreased, the critical temperatures associated with ε_n states ($n = 1, 2, \ldots$) are exceeded sequentially and, consequently, the Δ_n superconducting states become available one by one, each with a different spatial distribution of superconducting gaps among the interfaces. The actual solution of the nonlinearized GL equations (4) and (5) for Δ is a linear combination of the available eigenstates Δ_n, therefore, as the temperature decreases, one may find stable solutions where Δ contains contributions of higher n eigenstates that lead to nontrivial spatial distributions of the Cooper-pair condensate among the interfaces, as we will discuss in greater detail in the next section.

The numerically obtained ε_n eigenstates in the systems with 3 and 4 interfaces are plotted as solid lines in Figs. 5(a) and 5(b), respectively, for the weak DW suppression case. Results obtained with the tight-binding model, using hopping parameters given by Eq. (10), are shown as open symbols, where good agreement is observed only for interface separations beyond $d \approx 4\,\xi_w$. As previously discussed, the disagreement between the numerical and the tight-binding results for shorter d stems from the fact that, for small separations, the DW order parameter W decreases in the regions between the interfaces [see the inset of Fig. 3(a)], so that the problem of several interfaces with short separation can no longer be described as a combination of several single-interface problems in a tight-binding approach. For instance, in the case of 3 interfaces, even the intermediate eigenvalue state ε_1, which in the tight-binding model is a constant ε_0 for any d, starts to decrease as d becomes smaller in the actual system as a consequence of the decreasing $W(x)$ between the interfaces. This situation expectedly worsens in the strong DW suppression regime, and yields further departure of the approximate tight-binding model from the actual numerical results of Eq. (9), as shown in Figs. 5(c) and 5(d). The sharp kinks seen in these figures result from the strong suppression of DW in-between the interfaces at small separations d, similar to those observed for the two-interfaces case in Fig. 3(a). Nevertheless, the tight-binding model proposed here still yields a good quantitative prediction for $d > 4\,\xi_w$ in all cases, while preserving at least good qualitative predictions of the eigenvalues behavior in the weak-suppression regime even for smaller d.

The maximum value of the SC order parameter $\Delta_{\max,n}$ provides us an estimate of the superconducting gap at the interfaces. This value raises from zero as the temperature is decreased below the critical temperature of the nth eigenstate of Eq. (9). Notice that although Eq. (9) provides the critical temperature T_{cn} of each eigenstate, through the relation between the eigenvalue and the critical temperature $\varepsilon_n = \xi_r^2(1 - T_{cn}/T_\Delta)$, it does not provide the actual temperature dependence of each eigenstate $\Delta_{\max,n}$. In order to obtain this value, we solve Eq. (7) through a relaxation procedure for different temperatures. The result is shown in Fig. 6(a) and 6(b), plotting $\Delta_{\max,n}$ for the first three (four) states of a system with three (four) interfaces as a function of temperature.

At this point we can employ the reasonable reliability of our tight-binding model to extend our results to the case of $N \to \infty$ interfaces. For an arbitrary N, the proposed tight-binding matrix D assumes the tridiagonal Toeplitz form [40], whose eigenvalues are

$$\varepsilon_n = \varepsilon_0 - 2\tau(d)\cos\left(\frac{n\pi}{N+1}\right). \tag{11}$$

It is straightforward to verify that previous results for $N = 2$–4 are specific cases of this general expression. As $N \to \infty$, an infinite series of states form a band of eigenvalues $\varepsilon(k) = \varepsilon_0 - 2\tau(d)\cos(kd)$, limited within the range $[\varepsilon_0 - 2\tau, \varepsilon_0 + 2\tau]$. Consequently, there will be a range of critical temperatures so that, as the system cools down, a series of SC eigenstates at the interfaces sequentially become energetically favorable, for temperatures within this range. This is illustrated by the shaded area in Fig. 6(c). Most importantly, the upper bound of this range of critical temperatures is controlled by the strength of the coupling between interfaces τ, which depends, e.g., on the separation between the interfaces. This can thus be seen as a mechanism to effectively enhance critical temperature of interface superconductivity in a system consisting of a large number of parallel interfaces, as we will discuss further on. Notice that the critical temperatures obtained here are enhanced as compared to those expected either for a single interface or for multiple noncoupled interfaces (i.e., far apart from each other), although they are still smaller than the critical temperature expected for the same order parameter in the bulk case.

For instance, Fig. 7 shows the square modulus of the SC order parameter (Cooper-pair density) corresponding to the (a) first, (b) second, (c) third, and (d) fourth eigenstates of a $N = 10$ interfaces system. Different eigenstates exhibit diverse probability density distributions of Cooper pairs: the

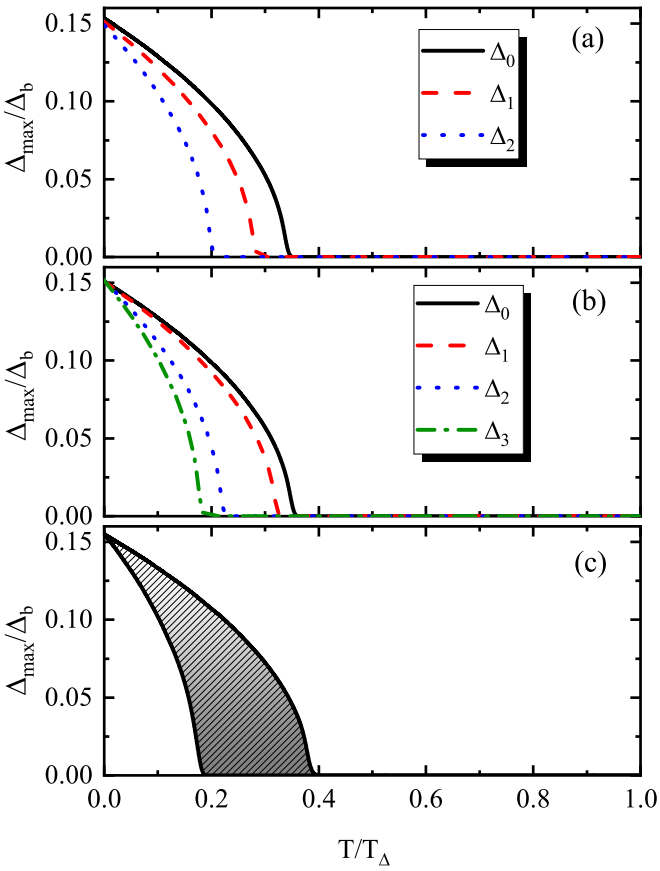

FIG. 6. Maximum values of the superconducting order parameter $\Delta_n(x)$ as a function of temperature, for the first (a) three eigenstates of a three-interfaces system, and (b) four eigenstates of a four-interfaces system. (c) The same as (a), (b), but for an infinite superlattice of equally spaced parallel interfaces. In all cases, interfaces are separated by $d = 3.5\,\xi_w$, assuming weak DW suppression $\alpha_0 = 1$.

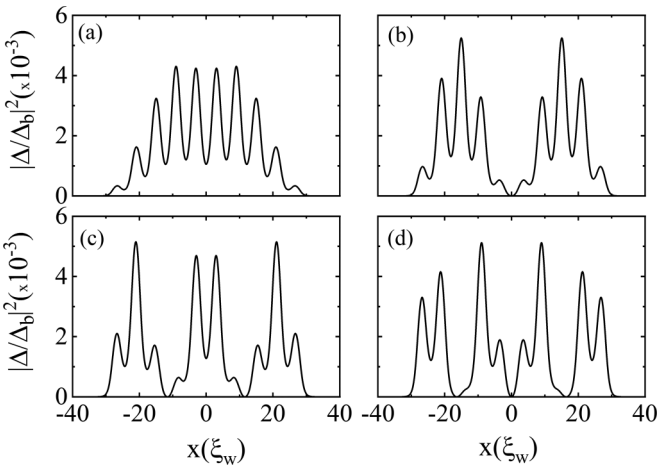

FIG. 7. The Cooper-pair density associated with eigenfunctions (a) Δ_0, (b) Δ_1, (c) Δ_2, and (d) Δ_3 of the SC order parameter in a system with 10 interfaces separated by $d = 3\,\xi_w$. The number of nodes, where the SC order parameter reaches zero in-between adjacent layers, increases with n, where each node coincides with a phase shift by π.

first eigenstate, with higher critical temperature, shows higher probability density in the central interfaces, and SC persists in-between the interfaces. For higher n, on the other hand, the odd-even nature of the eigenfunctions causes the SC order parameter to reduce to zero in-between some interfaces, due to appearance of the nodes in the order parameter (i.e., slips of phase by π). In Fig. 7(b), the eigenfunction for $n = 1$ exhibits zero SC order parameter at $x = 0$, effectively forming a π-Josephson junction between the left and the right sides of the 10-interfaces system. The number of such nodes increases with n, which is reminiscent of eigenfunctions in a finite square quantum well. Since for large interface separation d all the eigenstates are degenerate, i.e., having the same critical temperature, one expects to be able to observe stable nontrivial states such as those with SC stronger in some interfaces than in other, as well as states with π-Josephson junctions formed between some interfaces, as we discuss in what follows.

IV. SUPERCONDUCTING STATES AS A FUNCTION OF TEMPERATURE: THE COMPLETE SOLUTION

The solutions obtained from our linearized GL formalism suggest an interesting interplay of superconductivity among the interfaces, namely, there is a critical temperature degeneracy of different SC eigenstates if there is more than one interface, and this degeneracy is lifted as the interfaces are brought closer to each other. However, these results do not represent the complete solution of the GL equation. Actually, these states rather form a basis in which one can express the complete solutions. For instance, assuming only two interfaces, the complete solution can be written as a linear combination of Δ_0 and Δ_1 eigenstates. It is now important to discuss the impact of these eigenstates on the actual solution, i.e., as we consider the full nonlinear form of the GL equation for the SC order parameter. To answer this question, the coupled equations (4) and (5) are solved self-consistently using a relaxation method.

First, let us consider the simplest case of two interfaces. According to the eigenstates shown in Fig. 2(b), the complete solutions must be either symmetric, antisymmetric, or a combination of the two. Nevertheless, Fig. 3 shows that the symmetric and antisymmetric eigenstates have different critical temperature, depending of the separation d, with Δ_0 always having a higher critical temperature. Figure 8 shows the reduced temperature T/T_Δ below which the SC order parameter Δ emerges from zero. Notice that, in our model, if the sample was entirely superconducting, the reduced temperature where superconductivity appears is $T/T_\Delta = 1$. Instead, our sample is in the DW state, which competes with superconductivity and suppresses it across the system. It is the suppression of the DW order parameter at the interfaces that gives rise to superconductivity, and this is expected to occur at temperatures that are only a fraction of the critical temperature T_Δ. Indeed, interfaces separated by $d = 6\,\xi_w$ become superconducting at $T \approx 0.09T_\Delta$ in Fig. 8(a), whereas this effective critical temperature decreases to $T \approx 0.058T_\Delta$ and $\approx 0.052T_\Delta$ for larger separations $d = 12\,\xi_w$ and $40\,\xi_w$ in Figs. 8(b) and 8(c), respectively. In fact, this dependence of the effective SC critical temperature on the separation d is expected from

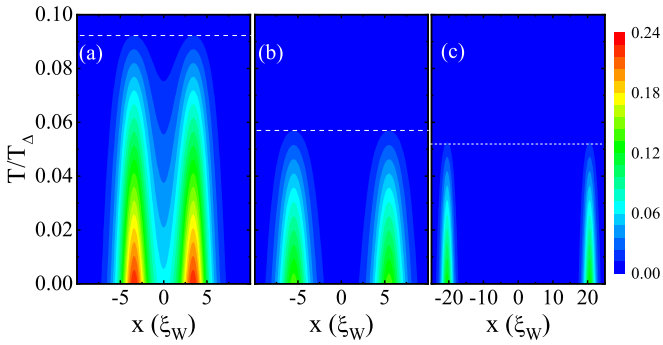

FIG. 8. Color maps of the Cooper-pair density Δ as a function of the reduced temperature T/T_Δ, calculated by the self-consistent solution of Eqs. (4) and (5), for two interfaces separated by (a) $d = 6\,\xi_w$, (b) $12\,\xi_w$, and (c) $40\,\xi_w$. For shorter separations, the SC order parameter in the interfaces is enhanced and the effective critical temperature, marked by the horizontal dashed lines, increases, in accordance with the predictions from the linearized GL formalism.

the results of the linearized equations: as the interfaces get closer, the critical temperature of the symmetric eigenstate Δ_0, which is the highest one, increases. This demonstrates the potentially practical enhancement of the SC critical temperature by creating superlattices with interfaces stacked closer together or, alternatively, by increasing the number of stacked interfaces, since the critical temperature of the eigenstate Δ_0 also increases with N, as verified in Fig. 6.

For further reduced temperature, the critical temperature of the antisymmetric eigenstate Δ_1 is reached, which triggers its role as a possible basis state for the SC order parameter. As both eigenstates are now achievable, solutions in the form $\Delta = a_0\Delta_0 + a_1\Delta_1$ are possible. A combination, e.g., with $a_0 = a_1$ results in superconductivity nucleating only in one interface. This is shown in Fig. 9(a), where a solution with superconductivity active only in one interface is found metastable up to $T/T_\Delta \approx 0.01$. Even at zero temperature, this solution is only stable when the interfaces are far from each other (beyond $35\xi_w$ in this case), so that the energies of either symmetric, antisymmetric, or a combination of the two eigenstates are practically the same. As the interfaces get closer, the single-interface SC state is no longer stable [see Fig. 9(b)]. This is due to the tunneling of Cooper pairs through the DW region that separates the interfaces, so that if one interface is superconducting, it induces superconductivity in the other interface as well.

The tight-binding model introduced in Sec. III predicts that the critical temperature of interface superconductivity increases with the number of stacked interfaces. Figure 10 illustrates three possible states found by solving the complete GL formalism for a system of $N = 10$ interfaces. Indeed, in all cases, the effective critical temperature of the system is significantly higher than those observed for the two-interface system in Fig. 8. The state shown in Fig. 10(a), obtained by relaxation of a spatially randomized initial trial function, has all interfaces exhibiting superconductivity at low temperatures, with slightly higher Cooper-pair densities in the inner interfaces than in the outer ones. As the temperature is increased, SC at the peripheral interfaces is suppressed first.

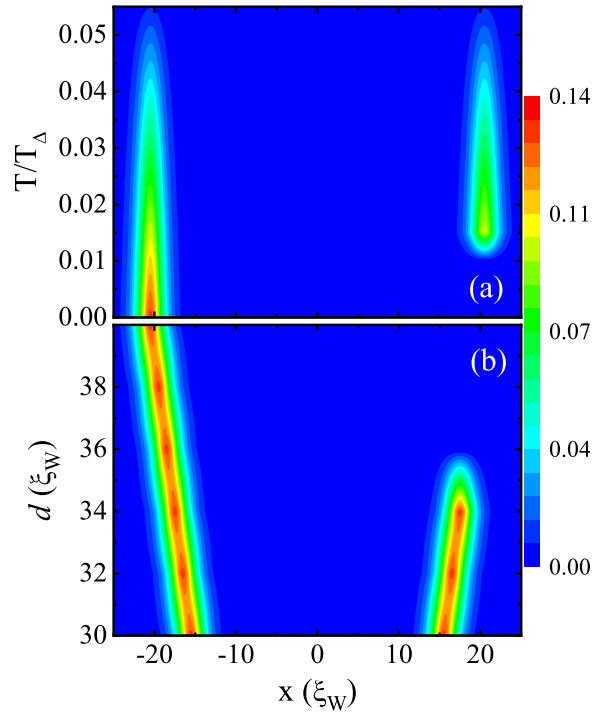

FIG. 9. Color map of the Cooper-pair density in two parallel interfaces, obtained by solving the full nonlinear GL set of equations, as a function of (a) temperature, for a fixed interface separation distance $d = 40\,\xi_w$, and (b) as a function of d, for a fixed temperature $T = 0$. The metastable solution where SC is active only in one of the interfaces (left) is obtained only for larger separation between the interfaces, and is expected to be experimentally achieved after a rapid quench to low temperatures.

Conversely, Figs. 10(b) and 10(c) exhibit stable states where SC is entirely suppressed in some of the inner interfaces. Indeed, as temperature is decreased, the critical temperatures of different SC eigenstates are reached, allowing several possible combinations of eigenfunctions with different numbers of spatial nodes and associated phase shifts. Consequently, at sufficiently low temperatures, there may exist stable

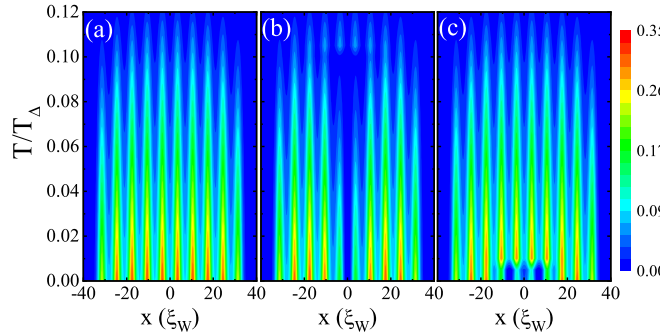

FIG. 10. Color map of the Cooper-pair density in 10 parallel interfaces separated by $d = 6\,\xi_w$, obtained by solving the full nonlinear GL set of equations as a function of temperature. (a)–(c) Exemplify three different metastable states at low temperatures, obtained after initialization from many different initial conditions (simulating nucleation from the normal state).

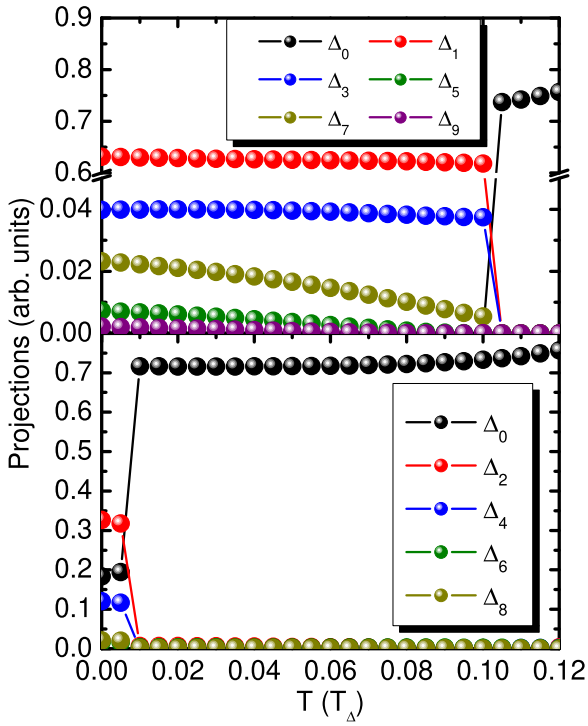

FIG. 11. Projections of the Cooper-pair densities shown in Fig. 10(b) (top panel) and Fig. 10(c) (bottom panel) on the eigenstates Δ_n of a system with 10 stacked interfaces.

solutions with Cooper-pair density suppressed in one or more interfaces, similar to what is observed in Fig. 9(a) for $N = 2$. These are actually metastable states (i.e., they are obtained by convergence of an initial arbitrary Δ in the relaxation procedure), but higher in energy than the state shown in Fig. 10(a), hence are less frequently obtained when starting the calculation from different initial conditions.[1] They remain, however, relevant towards experimental observation, especially upon rapid cooling to low temperatures from the normal state (so-called field-cooled regime).

Different combinations of involved eigenstates in the composition of the superconducting states in Figs. 10(b) and 10(c) are shown in the top and bottom panels of Fig. 11, respectively. Notice that the state in Fig. 10(a) is composed of only the ground eigenstate Δ_0 for any temperature and is therefore not shown in Fig. 11. On the other hand, the state in Fig. 10(b) results from a combination of eigenstates with odd index up to $T = 0.1T_\Delta$, where the Δ_0 state becomes dominant and the converged state resembles that of Fig. 10(a) for higher temperatures. Notice that the eigenstates with higher eigenvalues (i.e., lower critical temperature) contribute less to the state, especially for higher temperatures. The state with a strong suppression of SC at the inner interfaces for temperatures up to $T = 0.01T_\Delta$, shown in Fig. 10(c), is composed of the eigenstates with even indices, as shown in the bottom panel of Fig. 11.

We point out that such exotic states, where superconductivity is suppressed in specific interfaces, is a special case of latent superconductivity: the system is below the effective superconducting critical temperature and no competing order parameter is present in these interfaces since the DW is strongly suppressed in all interfaces. Even so, superconducting state may nucleate in nontrivial configurations across the interfaces, due to the specific combination of eigenstates of the system, where eigenfunctions with opposite phases may lead to (partial) cancellation of the SC order parameter at the inner interfaces. We also point out that the metastable exotic states discussed here are not expected to be experimentally achievable by simply slowly lowering the temperature, but rather only by rapid quenching the temperature to below the critical temperature of the exotic state. Such a rapid quench would lead to one of the metastable states at very low temperatures, so that Figs. 9 and 10 would thus capture the behavior of the order-parameter distribution upon slowly warming the system.

All results discussed here were made assuming a constant interface width. Nevertheless, it is straightforward to predict how a different interface width would affect our results and conclusions: within the linearized version of the theory in Eq. (9) and Sec. III, the suppression of the DW order parameter at the interface effectively acts like a quantum well, whereas the emergent modes of the SC order parameter at the interface play the role of confined eigenstates of that quantum well. Increasing the interface width would simply lead to more SC eigenstates in each interface, with lower eigenvalues ε [35]. Consequently, the formation of a band of SC modes discussed in Sec. III for a series of parallel interfaces still holds, but now there will be one band originating from each excited eigenstate of the interface as well, similar to the formation of bands due to a series of finite quantum wells in a superlattice. The thin interface width considered here guarantees that all possible excited bands in the system give negligible contribution to the SC states numerically obtained with Eqs. (4) and (5) and discussed in Sec. IV. This choice was made for the sake of clarity of the results in Figs. 9–11, where, indeed, only the states Δ_n originating from the ground state of the isolated interface play a significant role. In the case of thicker interfaces, due to the lower eigenvalues of the series of states stemming from the excited states of each interface, more eigenstates may significantly contribute to the SC order parameter in Figs. 9–11, beyond the Δ_n states series, which may lead to even more exotic spacial distributions of the latent SC state. Nevertheless, qualitatively, all conclusions drawn here, especially regarding the existence of metastable states where SC is suppressed in some interfaces due to interference, remain valid.

V. CONCLUSIONS

In summary, we have employed a two-component GL model to investigate properties of superconductivity arising in competition with another dominant (spin and charge density) order in a series of parallel interfaces. The model is developed on top of the one previously proposed in Ref. [35], where two

[1]Results in Figs. 10(b) and 10(c) are obtained by relaxation of initial order-parameter functions with specific symmetries: they are given by a random number distribution multiplied by $\sin(\pi x/L_T)$ and $\sin(2\pi x/L_T)$ backgrounds, respectively, where L_T is the length of the computational box.

competing order parameters exhibit density-density coupling, but is easily extendable to other coupling forms stemming from a microscopic derivation. We go beyond this previous model by expanding its concept to the case of several parallel interfaces, where we demonstrate that as more interfaces are stacked together, the number of possible superconducting states across these interfaces increases as well, each with a different critical temperature. The critical temperature of the ground state, which would thus be the superconducting critical temperature of the system, depends on the distance between interfaces, on the number of stacked interfaces and, generally speaking, on the coupling between adjacent interfaces. Bearing in mind the large number of systems where interface superconductivity is relevant, especially the artificially fabricated ones, our study conveniently indicates pathways towards control of critical temperature by nanoengineering of material superlattices.

Different (meta)stable superconducting states we found in the superlattice of interfaces are not only rich in number, but also in different physical manifestation, since some of them can host rather nontrivial spatial distribution of the Cooper-pair condensate, and even contain intrinsic π-Josephson junctions between parts of the superlattice. That suggests very rich possible behavior of the system in applied current and/or magnetic field, worthy of further exploration.

ACKNOWLEDGMENTS

This work was supported by the Conselho Nacional de Desenvolvimento Científico e Tecnológico (CNPq), under the PQ program, PRONEX/FUNCAP and CAPES foundation, and the Research Foundation-Flanders (FWO).

[1] P. N. Chubov, V. V. Eremenko, and Yu. A. Pilipenko, Zh. Eksp. Teor. Fiz. **55**, 752 (1968) [Sov. Phys. JETP **28**, 389 (1969)].
[2] V. G. Kogan and N. Nakagawa, Phys. Rev. B **35**, 1700 (1987).
[3] E. F. Talantsev, W. P. Crump, J. O. Island and Y. Xing, Y. Sun, J. Wang, and J. L. Tallon, 2D Mater. **4**, 025072 (2017).
[4] Y. Yang, S. Fang, V. Fatemi, J. Ruhman, E. Navarro-Moratalla, K. Watanabe, T. Taniguchi, E. Kaxiras, and P. Jarillo-Herrero, Phys. Rev. B **98**, 035203 (2018).
[5] E. Montevecchi and J. O. Indekeu, Europhys. Lett. **51**, 661 (2000).
[6] M. Mito, H. Matsui, K. Tsuruta, T. Yamaguchi, K. Nakamura, H. Deguchi, N. Shirakawa, H. Adachi, T. Yamasaki, H. Iwaoka, Y. Ikoma, and Z. Horita, Sci. Rep. **6**, 36337 (2016).
[7] M. Abdel-Hafiez, X.-M. Zhao, A. A. Kordyuk, Y.-W. Fang, B. Pan, Z. He, C.-G. Duan, J. Zhao, and X.-J. Chen, Sci. Rep. **6**, 31824 (2016).
[8] O. Cyr-Choinière, D. LeBoeuf, S. Badoux, S. Dufour-Beauséjour, D. A. Bonn, W. N. Hardy, R. Liang, D. Graf, N. Doiron-Leyraud, and L. Taillefer, Phys. Rev. B **98**, 064513 (2018).
[9] X. Yang, Y. Zhou, M. Wang, H. Bai, X. Chen, C. An, Y. Zhou, Q. Chen, Y. Li, Z. Wang, J. Chen, C. Cao, Y. Li, Y. Zhou, Z. Yang, and Z. Xu, Sci. Rep. **8**, 6298 (2018).
[10] M. Krishnan, R. Pervin, K. S. Ganesan, K. Murugesan, G. Lingannan, A. K. Verma, P. M. Shirage, and A. Sonachalam, Sci. Rep. **8**, 1251 (2018).
[11] A. Gabovich, A. Voitenko, T. Ekino, M. S. Li, H. Szymczak, and M. Pekala, Adv. Condens. Matter Phys. (2010) 681070.
[12] P. Dai, Rev. Mod. Phys. **87**, 855 (2015).
[13] K. Cho, M. Kończykowski, S. Teknowijoyo, M. A. Tanatar, J. Guss, P. B. Gartin, J. M. Wilde, A. Kreyssig, R. J. McQueeney, A. I. Goldman, V. Mishra, P. J. Hirschfeld, and R. Prozorov, Nat. Commun. **9**, 2796 (2018).
[14] P. Cai, X. Zhou, W. Ruan, A. Wang, X. Chen, D.-H. Lee, and Y. Wang, Nat. Commun. **4**, 1596 (2013).
[15] F. L. Ning, K. Ahilan, T. Imai, A. S. Sefat, M. A. McGuire, B. C. Sales, D. Mandrus, P. Cheng, B. Shen, and H.-H. Wen, Phys. Rev. Lett. **104**, 037001 (2010).
[16] D. K. Pratt, W. Tian, A. Kreyssig, J. L. Zarestky, S. Nandi, N. Ni, S. L. Budko, P. C. Canfield, A. I. Goldman, and R. J. McQueeney, Phys. Rev. Lett. **103**, 087001 (2009).
[17] H. Chen, Y. Ren, Y. Qiu, W. Bao, R. H. Liu, G. Wu, T. Wu, Y. L. Xie, X. F. Wang, Q. Huang, and X. H. Chen, Europhys. Lett. **85**, 17006 (2009).
[18] R. Gupta, U. B. Paramanik, S. Ramakrishnan, K. P. Rajeev, and Z. Hossain, J. Phys.: Condens. Matter **28**, 195702 (2016).
[19] R. Gupta, S. K. Dhar, A. Thamizhavel, K. P. Rajeev, and Z. Hossain, J. Phys.: Condens. Matter **29**, 255601 (2017).
[20] B. Leridon, S. Caprara, J. Vanacken, V. V. Moshchalkov, B. Vignolle, R. Porwal, R. C. Budhani, A. Attanasi, M. Grilli, and J. Lorenzana, New J. Phys. **22**, 073025 (2020).
[21] H. Miao, G. Fabbris, R. J. Koch, D. G. Mazzone, C. S. Nelson, R. Acevedo-Esteves, G. D. Gu, Y. Li, T. Yilimaz, K. Kaznatcheev *et al.*, npj Quantum Mater. **6**, 31 (2021).
[22] S. J. Denholme, A. Yukawa, K. Tsumura, M. Nagao, R. Tamura, S. Watauchi, I. Tanaka, H. Takayanagi, and N. Miyakawa, Sci. Rep. **7**, 45217 (2017).
[23] A. Chikina, A. Fedorov, D. Bhoi, V. Voroshnin, E. Haubold, Y. Kushnirenko, K. H. Kim, and S. Borisenko, npj Quantum Mater. **5**, 22 (2020).
[24] Y. Kvashnin, D. VanGennep, M. Mito, S. A. Medvedev, R. Thiyagarajan, O. Karis, A. N. Vasiliev, O. Eriksson, and M. Abdel-Hafiez, Phys. Rev. Lett. **125**, 186401 (2020).
[25] C.-S. Lian, C. Si, and W. Duan, Nano Lett. **18**, 2924 (2018).
[26] Q. L. He, H. Liu, M. He, Y. H. Lai, H. He, G. Wang, K. T. Law, R. Lortz, J. Wang, and I. K. Sou, Nat. Commun. **5**, 4247 (2014)
[27] A. Frano, S. Blanco-Canosa, E. Schierle, Y. Lu, M. Wu, M. Bluschke, M. Minola, G. Christiani, H. U. Habermeier, G. Logvenov, Y. Wang, P. A. van Aken, E. Benckiser, E. Weschke, M. Le Tacon, and B. Keimer, Nat. Mater. **15**, 831 (2016).
[28] M. S. Scheurer, and J. Schmalian, Nat. Commun. **6**, 6005 (2015).
[29] D. T. Harris, N. G. Campbell, C. Di, J. M. Park, L. Luo, H. Zhou, G. Y. Kim, K. Song, S. Y. Choi, J. Wang, M. S. Rzchowski, and C. B. Eom, Phys. Rev. B **101**, 064509 (2020).

[30] C. Boix-Constant, S. Mañas-Valero, R. Córdoba, and E. Coronado, Adv. Electron. Mater. **7**, 2000987 (2021).

[31] A. J. Li, X. Zhu, G. R. Stewart, and A. F. Hebard, Sci. Rep. **7**, 4639 (2017).

[32] C.-S. Lian, C. Heil, X. Liu, C. Si, F. Giustino, and W. Duan, J. Phys. Chem. Lett. **10**, 4076 (2019).

[33] E. Navarro-Moratalla, J. O. Island, S. Mañas-Valero, E. Pinilla-Cienfuegos, A. C. Gomez, J. Quereda, G. Rubio-Bollinger, L. Chirolli, J. A. Silva-Guillén, N. Agraït, G. A. Steele, F. Guinea, H. S. J. van der Zant, and E. Coronado, Nat. Commun. **7**, 11043 (2016).

[34] C. Chen, L. Su, A. H. Castro Neto, and V. M. Pereira, Phys. Rev. B **99**, 121108(R) (2019).

[35] A. Moor, A. F. Volkov, and K. B. Efetov, Phys. Rev. B **91**, 064511 (2015).

[36] A. Moor, P. A. Volkov, A. F. Volkov, and K. B. Efetov, Phys. Rev. B **90**, 024511 (2014).

[37] M. G. Vavilov, A. V. Chubukov, and A. B. Vorontsov, Supercond. Sci. Technol. **23**, 054011 (2010).

[38] A. B. Vorontsov, M. G. Vavilov, and A. V. Chubukov, Phys. Rev. B **81**, 174538 (2010).

[39] R. M. Fernandes and J. Schmalian, Phys. Rev. B **82**, 014521 (2010).

[40] S. Noschese, L. Pasquini, and L. Reichel, Numer. Linear Algebra Appl. **20**, 302 (2013).